OPEN

PRS GLOBAL OPEN

ORIGINAL ARTICLE
Research

In Vivo Perforasome Perfusion in Hemi-DIEP Flaps Evaluated with Indocyanine-green Fluorescence Angiography and Infrared Thermography

Muiz A. Chaudhry, MD*†
James B. Mercer, PhD†‡§
Louis de Weerd, MD, PhD*†

Background: There are no in vivo studies that evaluate the effect of perforator dissection on the perfusion territory of a perforator (perforasome). In this study, indocyanine green fluorescence angiography (ICG-FA) and infrared thermography (IRT) were used intraoperatively to evaluate perforasome perfusion in hemi-DIEP flaps.
Methods: Patients selected for DIEP breast reconstruction were prospectively included in the study. Preoperative perforator mapping was performed with CTA and handheld Doppler ultrasound. In general anesthesia, perforasome perfusion was evaluated with ICG-FA and IRT both before surgery and after flap dissection with preserved dominant perforators.
Results: Thirty hemi-DIEP flaps were dissected in 15 patients (average BMI 26.6 kg/m^2), of which 40% had been operated on in the lower abdomen. Fluorescence spots from ICG were associated with infrared radiation hotspots on IRT and these corresponded with the locations of the selected perforators. IRT and ICG-FA demonstrated similar patterns in perforasome perfusion before and after perforator dissection. Perforator dissection changed the perforasome perfusion. IRT made it possible to continuously monitor the perforator activity during surgery. ICG-FA easily identified areas with impaired flap perfusion due to previous surgery.
Conclusions: Perforasome perfusion is a dynamic process that changes with perforator dissection. ICG-FA and IRT are reproducible techniques for in vivo evaluation of perforasome perfusion and produce comparable results. *(Plast Reconstr Surg Glob Open 2021;9:e3560; doi: 10.1097/GOX.0000000000003560; Published online 21 May 2021.)*

*From the *Department of Plastic and Reconstructive Surgery, University Hospital of North Norway, Tromsø, Norway; †Medical Imaging Research Group, Department of Clinical Medicine, UiT, The Arctic University of Norway, Tromsø, Norway; ‡Department of Radiology, University Hospital of North Norway, Tromsø, Norway; and §Department of Medical Biology, UiT, The Arctic University of Norway, Tromsø, Norway.*

Received for publication January 31, 2021; accepted February 22, 2021.

An abstract with preliminary results has been presented at annual meeting of the Norwegian Association of Plastic Surgeons in 2019, Oslo, Norway. The same abstract was awarded second best price on the 25th jubilee meeting of Pakistan Asssociation of Plastic Surgeons (PAPS CON) 2020, Islamabad, Pakistan. An abstract from this paper is accepted for oral presentation at annual meeting of European Association of Plastic Surgery (EURAPS) 2020 Athens, Greece.

Copyright © 2021 The Authors. Published by Wolters Kluwer Health, Inc. on behalf of The American Society of Plastic Surgeons. This is an open-access article distributed under the terms of the Creative Commons Attribution-Non Commercial-No Derivatives License 4.0 (CCBY-NC-ND), where it is permissible to download and share the work provided it is properly cited. The work cannot be changed in any way or used commercially without permission from the journal.

DOI: 10.1097/GOX.0000000000003560

INTRODUCTION

The deep inferior epigastric perforator (DIEP) flap has become the first choice in autologous breast reconstruction, as excellent aesthetic results can be obtained with minimal donor site morbidity. However, rates of fat necrosis for DIEP breast reconstruction may be as high as 35%, which not only reduces the aesthetic result but also causes uncertainty due to lump formation in the reconstructed breast.[1,2] Fat necrosis is a result of inadequate flap perfusion. Selection of a suitable perforator is critical for decreasing the rate of postoperative fat necrosis and minimizing perfusion-related flap complications.[3] A thorough understanding of the vascular anatomy and flow characteristics of a selected perforator is essential to balance flap design and adequate flap perfusion. The angiosome concept by Taylor and Palmer has greatly contributed to our knowledge on flap perfusion.[4] Saint-Cyr et al introduced in 2009 the perforasome theory and defined a perforasome as the territory perfused by a single perforator vessel of a named artery.[5] The importance of finding the most suitable perforator is reflected in the

Disclosure: *The article processing charge was funded by a grant from the publication fund of UiT, The Arctic University of Norway.*

large number of studies on the use of preoperative perforator mapping using imaging techniques.[6] Still the relationship between the designed flap size and areas of perfusion from the selected perforator is a clinical challenge because this ratio is unknown.[7] To our knowledge there are no in vivo studies that evaluate how the reduction of the number of perforators during flap harvest effects the perfusion area of a selected perforator.

Indocyanine green fluorescence angiography (ICG-FA) is an invasive technique that allows for direct visualization of tissue perfusion by registration of intravascular fluorescence intensity. Infrared thermography (IRT) is a noninvasive technique that indirectly visualizes skin perfusion by measuring infrared (IR) radiation released from the skin surface. In static infrared thermography (SIRT), a single image is taken from the area of interest. In dynamic infrared thermography (DIRT), the area of interest is exposed to a mild thermal challenge, and the rate and pattern of temperature changes are recorded and analyzed. ICG-FA and IRT are well-established techniques that provide real-time assessment of skin perfusion and have been shown to provide valuable information for perforator mapping.[7–12] The primary aim of this study was to evaluate the effect of perforator dissection on the perfusion area of the selected perforator in a hemi-DIEP flap by using ICG-FA and IRT intraoperatively. The secondary aim of this study was to compare the results from ICG-FA with those obtained from IRT with respect to flap perfusion.

MATERIALS AND METHODS

The study was approved by the Regional Committee for Medical and Health Research Ethics (REK Nord, approval number 2017/1641), institutional protection officer (DPO approval number 02369), and registered in ClinTrials.gov (NCT04115995). Fifteen female patients scheduled for secondary DIEP breast reconstruction were included in the study. Exclusion criteria were lactating women, smokers, body mass index (BMI) over 30 kg/m^2, renal or hepatic failure and previous history of reactions on ICG or iodine contrast.

On the lower abdomen, a hemi-DIEP flap was designed on each side of the midline. Preoperative perforator mapping was performed with a 128 × 2-slice dual-source computed tomographic angiography (CTA-SOMATOM Definition FLASH, Siemens Healthineers, Erlangen, Germany) and hand-held unidirectional Doppler ultrasound (8 MHz, Multi Dopplex II, Huntleigh Healthcare, Cardiff, UK). Arterial Doppler sound locations were marked with a permanent marker on the skin in a quadrant system overlying each rectus abdominis muscle.

Perfusion examinations (E1) of the hemi-DIEP flaps with ICG-FA and IRT were performed simultaneously after induction of general anesthesia and before surgery. Several perforators were selected for dissection based on preoperative imaging and intraoperative findings and were tested for Doppler sounds. The second examination (E2) was performed after the supra-fascial dissection of the selected perforators had been completed and with the superficial inferior epigastric vein (SIEV) open if found.

For ICG-FA, a video camera (IC-VIEW PULSION Medical Systems, Munich, Germany) was used. ICG binds exclusively to plasma proteins, is rapidly excreted into the bile, and has a plasma half-life of 3–4 minutes in healthy adults. After illumination of ICG with laser (energy p = 0.16 W, wavelength ≥780 nm), it induces near-infrared light (NIR, max spectral range 805 nm, fluorescence emission at 835 nm), which is recorded by the camera. Before each recording, the camera was calibrated to a fluorescence reference card. For ICG-FA, a bolus of 1.0 mg/kg (5mg ICG /1 ml saline) was injected intravenously. Recordings lasted until fluorescence was seen at the flap edge.

For IRT, an IR camera (FLIR ThermaCAM S65 HS FLIR Systems; FLIR Systems AB, Boston, Mass.) with a sensitivity of 0.1°C was used. Thermal emissivity was set to 0.98, and the camera accuracy was regularly checked against a black body with a traceable temperature source (Model IR-2103/301, Infrared Systems Development Corp., Winter Park, Fla.).

The IR- and ICG-FA cameras were mounted beside each other on an extendable boom of a specially designed camera stand, the height of which could be electronically controlled. With this system the lenses of both cameras could be positioned above and perpendicular to the exposed abdominal surface at a distance of 40 cm and 70 cm for the ICG-FA and IRT measurements, respectively.

In E2, DIRT was performed after the SIRT and ICG-FA examinations by exposing the skin to a mild cold challenge by placing a metal plate at room temperature (23–24°C) for 30 seconds on the skin. Skin rewarming was recorded for 3 minutes. The effect of closing SIEV or a selected perforator on flap perfusion was also evaluated. Images were digitally stored and processed using image analysis software ThermaCAM Researcher Pro 2.8 SR-1 (FLIR Systems AB, Boston, Mass.). The rate and pattern of rewarming of the skin were analyzed.

RESULTS

In 15 women, a mean age 52 years (range 32–76) and mean BMI of 26.9 kg/m^2 (range 24–30) 30 hemi-DIEP flaps were designed. Six patients (40%) had been previously operated on the lower abdomen, but only a few had a scar within the quadrant system. See Table 1 for patient and surgery data. The hemodynamic conditions were stable during E1 and E2 (Figs. 1, 2), and the room temperature in the operation theater was 24°C.

Table 1. Patient and Surgery Data

Patients:	**15 women**
Age, y [range]:	52 [32–76]
BMI [range]:	26.9 kg/m^2 [24–30]
Previous surgery in lower abdomen:	40.0% (6/15)
Indication for surgery:	12 breast cancers 3 BRCA gene mutation
No. hemi-DIEP flaps evaluated with SIRT & ICG-FA:	30

Note that 6 of the 15 patients (40 %) had been previously operated in the lower abdomen with either open surgery or a laparoscopic procedure (appendectomy, salpingo-oophorectomy, laparoscopic hemicolectomy, and caesarean section).

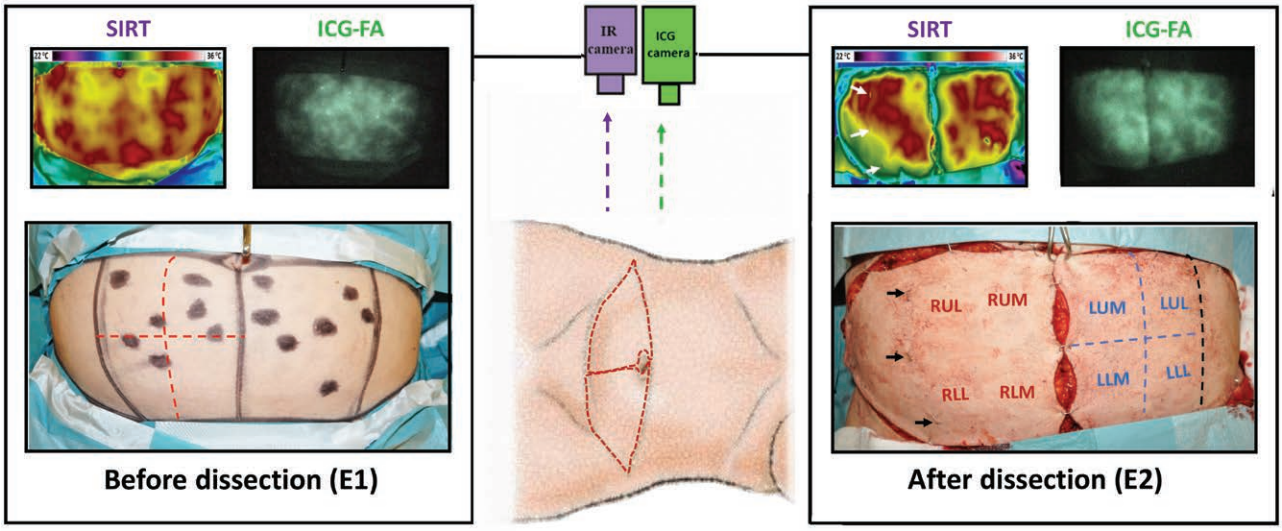

Fig. 1. Schematic presentation of the protocol for in vivo perfusion imaging of hemi-DIEP flaps in general anaesthesia before (E1) and after dissection of dominant perforators (E2). In each patient, SIRT and ICG-FA were performed simultaneously in E1 and E2. The IR- and ICG-FA cameras were mounted beside each other on the end of an extendable boom of a specially designed camera stand whose height could be electronically controlled. With this system, the lenses of both cameras could be positioned above and perpendicular to the exposed abdominal surface at a distance of 40 cm and 70 cm for the ICG-FA and IRT measurements, respectively. On the photographic images the system we used to divide the flap surface over each rectus fascia into four equal quadrants is indicated by the red (E1) and blue (E2) dashed lines. The lateral margins of the rectus muscle were marked with 3 staples in the skin (black arrows), which were easily visible on the SIRT images (white arrows) and facilitated orientation of perfusion spots after flap transfer. SIRT, static infrared thermography; ICG-FA, indocyanine green fluorescence angiography; RUL, right upper lateral; RUM, right upper medial; RLL, right lower lateral; RLM, right lower medial; LUM, left upper medial; LUL, left upper lateral; LLM, left lower medial; LLL, left lower lateral; E1, first dynamic imaging evaluations; E2, second dynamic imaging evaluations.

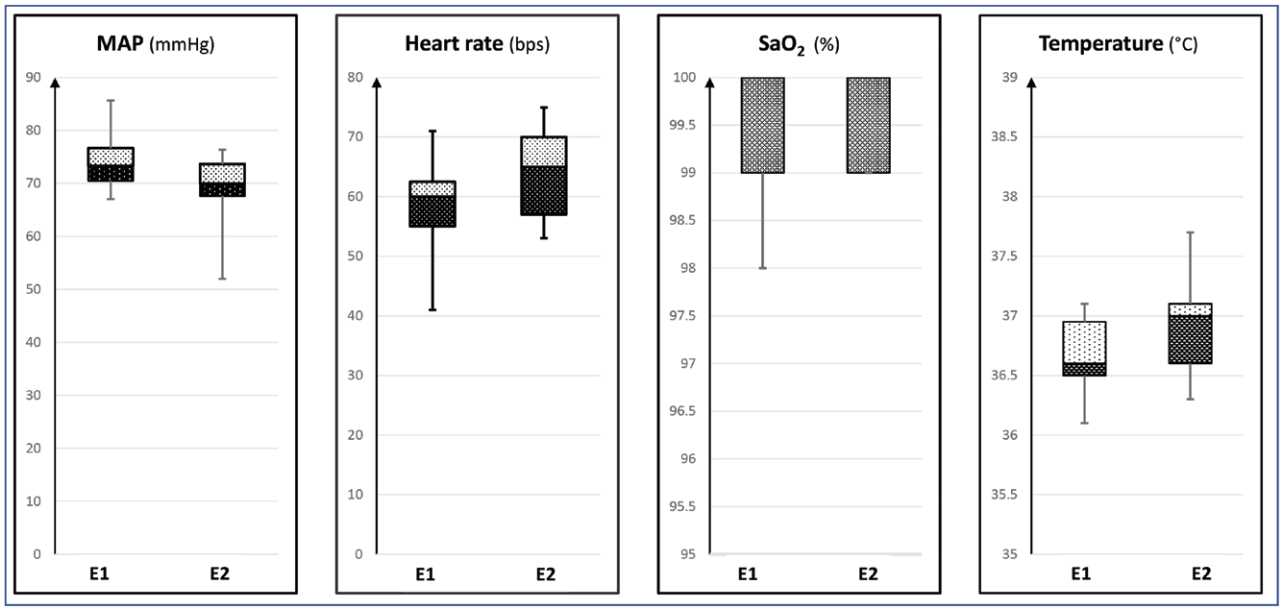

Fig. 2. Boxplots of hemodynamic values and body temperature at E1 and E2 during SIRT and ICG-FA examinations for all 15 patients. E1, SIRT and ICG-FA in general anesthesia but before surgery; E2, SIRT and ICF-FA in general anesthesia and after perforator dissection of hemi-DIEP flaps; SaO_2, Oxygen saturation.

First Examination (E1) with SIRT and ICG-FA

Thermographic images showed skin surface areas with continuous high IR radiation, called "hotspots." ICG-FA gave a short-lasting image of first appearing fluorescence spots and their subcutaneous branching network connecting associated fluorescence spots, before the dye rapidly reached the subdermal plexus and was distributed into the entire flap surface. The locations of IR hotspots and patterns of increased IR radiation were comparable with locations of fluorescence spots and their associated fluorescence patterns. Both imaging modalities showed a similar large variability in number, size, and locations of the fluorescence and IR patterns between both hemi-DIEP flaps for each patient, but also between patients. In contrast to SIRT, ICG-FA visualized more clearly a branching network between fluorescence spots and showed the dynamic changes within this network. On the other hand, SIRT visualized hotspots with a clearer border, especially in the lateral parts of the flap, where ICG always appeared less pronounced due to limited spread of the laser beam (Figs. 3–6).

Second Examination (E2) with SIRT and ICG-FA

After perforator dissection, both the patterns of the IR hotspots with IR radiation and fluorescence spots with their branching network changed dramatically compared with E1. Each remaining perforator was associated with the new perfusion pattern of fluorescence and IR radiation. The location of the first appearing fluorescence spot and high IR hotspot was always associated with the perforators exit point through the rectus abdominis fascia. IR radiation patterns associated with the selected perforators were clearly marked from each other by areas with lower IR radiation. Similarly, the fluorescence spots and branching network were surrounded by a clearly hypo-fluorescent bordered area. IRT confirmed increase in the size of the hotspot and ICG-FA visualized more clearly fluorescence accumulation in the localized remaining perfusion areas on E2 (Figs. 3, 4). ICG-FA rapidly showed a clear branching pattern that could not be seen on IRT, which stabilized into an IR radiation area of a certain size only after a few minutes. While the IRT pattern remained over time, the fluorescence pattern only lasted for a short time until ICG reached the subdermal

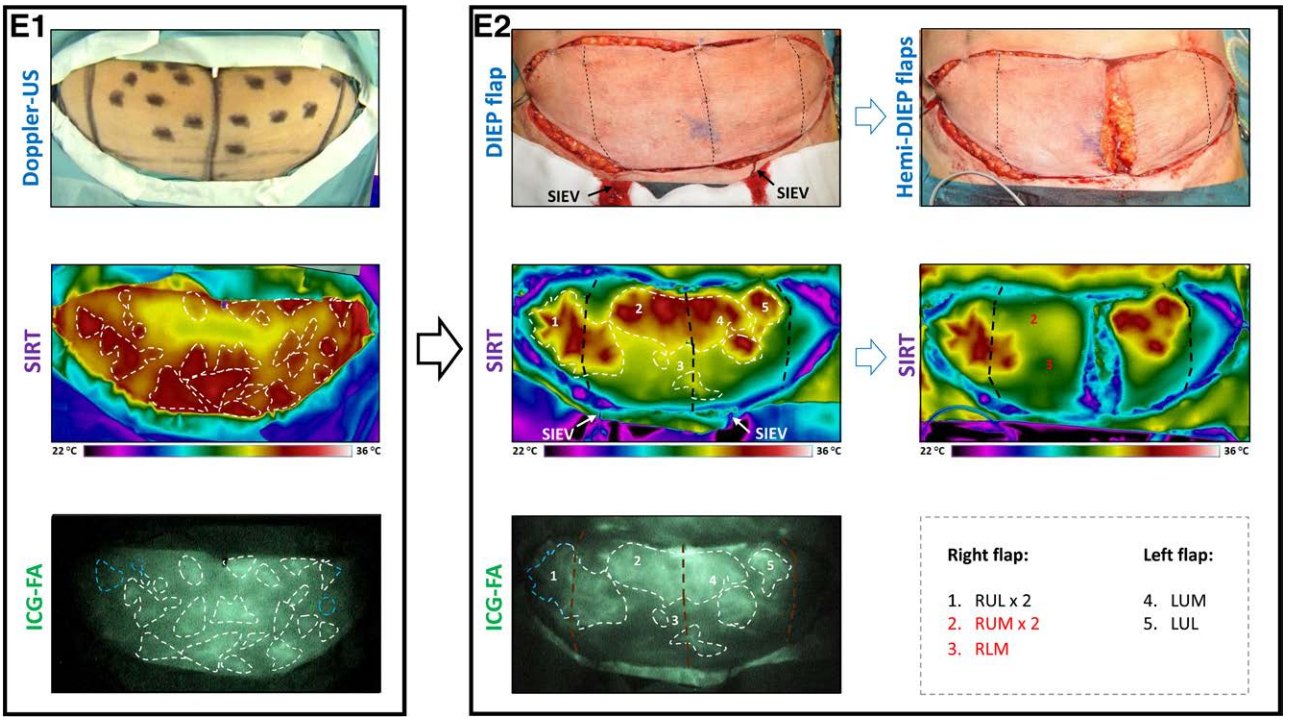

Fig. 3. In-vivo perfusion images showing the effect of perforator dissection in a 66 years old female. Left box: Results from E1. The locations of arterial Doppler sounds on both hemi-DIEP flaps are marked with black dots on the skin. The areas of increased IR radiation on SIRT and fluorescence on ICG-FA are highlighted with white dashed lines. Right box: Changes in the perfusion patterns after perforator dissection (E2) in 2 steps; first a DIEP flap with 7 preserved perforators (left side of box) and for 2 hemi-DIEP flaps with 5 remaining perforators (right side of box). Six of the seven selected dominant perforators were located in the upper quadrants. This could also be demonstrated with shift of IR hotspots and fluorescence spots to the upper part of the DIEP flap after perforator dissection. Further dissection of perforators (red number and text – left row) affected the respective IR radiation areas in the hemi-DIEP flaps. Perfusion patterns on SIRT and ICG-FA were comparable in E1 & E2, except in the lateral parts of the ICG-FA image (blue dashed line) due to limited spread of the laser beam. The identification and position of the perforators selected after flap dissection are identified with a number and an abbreviation (dashed line framed box in right corner). E1, dynamic imaging before surgery; E2, intraoperative dynamic imaging evaluations; Doppler US, Doppler ultrasound; SIRT, static infrared thermography; ICG-FA, indocyanine green fluorescence angiography; IR, infrared; SIEV, superficial inferior epigastric vein; RUL, right upper lateral; RUM, right upper medial; RLM, right lower medial; LUM, left upper medial; LUL, left upper lateral.

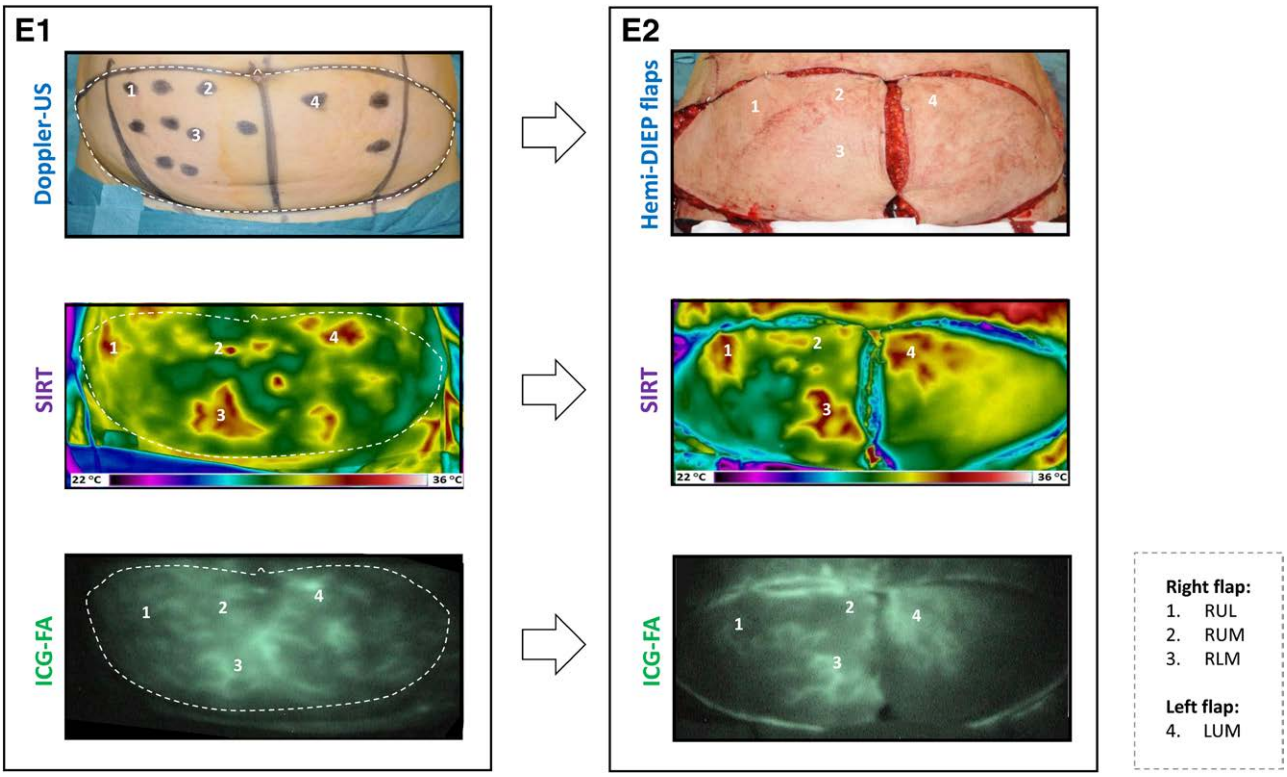

Fig. 4. Real-time perfusion images obtained before and after perforator dissection in a 53 years old patient. Each dominant perforator selected during flap dissection is identified with a number and an abbreviation (dashed line framed box in right corner). Left box: Results from Doppler ultrasound marking (black dots) on the lower abdomen and comparable perfusion pattern demonstrated with SIRT and ICG-FA on E1. Right box: Perfusion patterns visualized with SIRT and ICG-FA on E2 in both hemi-DIEP flaps. Note the increased IR radiation around the hotspots and wider branching pattern on ICG-FA when the flap is perfused by a single perforator (perforator no. 4 – LUM on E2). This could be due to increased inflow in the selected perforator from source artery when other perforators were cut. E1, evaluation before surgery; E2, evaluation after perforator dissection; Doppler US, Doppler ultrasound; SIRT, static infrared thermography; ICG-FA, fluorescence angiography of indocyanine green; IR, infrared; RUL, right upper lateral; RUM, right upper medial; RLM, right lower medial; LUM, left upper medial.

plexus and thereafter drained through the open end of the SIEV. High IR radiation from blood draining at the end of SIEV was also seen on IRT. In patients with abdominal scars, there were areas with no or minimal fluorescence uptake that went laterally from the scars after perforator dissection and remained hypo-fluorescent even when the dye reached the SIEV. In these areas, IR radiation was low but higher than room temperature (Figs. 5, 6).

DIRT and Clamping of Perforators

DIRT allowed for a continuously real-time monitoring of IR radiation from the flap surface. Clamping of a selected perforator followed by release of the clamp made it easy to identify the area and pattern of increased IR radiation associated with this perforator. Each perforator had a specific rewarming pattern that returned after release of the clamp. It was thus possible to identify the first appearing IR hotspot and associated IR hotspots. Clamping of a perforator had a variable effect on the rate and patterns of rewarming of the flap. In some cases, clamping of a lateral row perforator resulted in a disappearance of the associated hotspot and an increase in the rate and pattern of rewarming of the remaining perforators and visa versa (Figs. 7, 8). However, in other cases, clamping of a perforator did not result in a change in the overall thermal pattern. If DIRT showed high IR from the open end of SIEV, clamping the superficial vein resulted in a change of the pattern and rate of rewarming of the IR hotspots in the flap surface (Fig. 7).

DISCUSSION

This study shows for the first time in vivo the effect perforator dissection has on the flow characteristics and vascular territory of the selected perforator in a hemi-DIEP flap. Another important finding is that the noninvasive technique IRT and invasive technique ICG-FA provide comparable information on the dynamic changes that occur in a hemi-DIEP flap after perforator dissection.

Studies have shown that ICG-FA and IRT can be used for perforator mapping.[8–10,12] In our study, the locations of fluorescence spots were associated with locations of IR hotspots in both E1 and E2. Following perforator dissection (E2), first appearing fluorescence spots were associated with first appearing IR hotspots on DIRT and the perforator's exit point at the rectus abdominis fascia. Onoda et al found a good correlation between perforator mapping with CTA and ICG-FA.[13] Perstana and Zenn

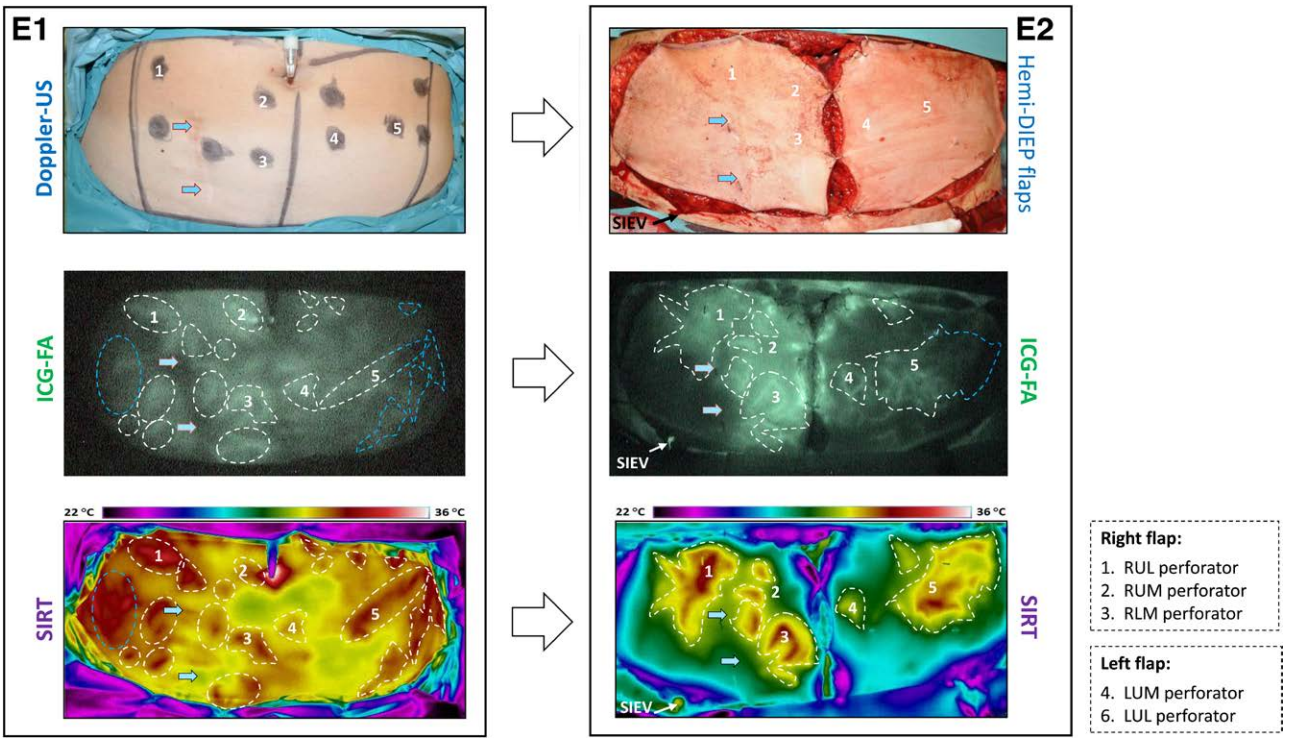

Fig. 5. The effect of perforator dissection revealed by real time perfusion images in a 47- years old female who had scars on the lower abdomen after appendectomy and laparoscopic surgery. Each dominant perforator selected during flap dissection is identified with a white number and an abbreviation (dashed line framed box in right corner). Left box: The results from E1. The locations of arterial Doppler sounds on both hemi-DIEP flaps were marked with black dots on the skin. The areas of increased fluorescence on ICG-FA and IR radiation on SIRT are highlighted with white dashed lines. Note the lack of fluorescence uptake in the McBurney scar (blue arrows). Based on her medical history and results from E1, a left sided hemi-abdominal flap was initially planned for her unilateral breast reconstruction. Right box: Radical changes in perfusion patterns after perforator dissection in both hemi-DIEP flaps. Due to such findings, the surgical plan was changed intraoperatively to select the right hemi-DIEP flap for the breast reconstruction. Areas with less ICG uptake and low IR radiation (E2) were trimmed off the flap and no perfusion related complications were reported in this patient. The perfusion patterns of both modalities were comparable, except in the lateral parts of the ICG-image (blue dashed line) due to limited spread of the laser beam. Selected periumbilical perforators after dissection (on E2) were draining into the SIEV. E1, evaluation before surgery; E2, evaluation after perforator dissection; Doppler US, Doppler ultrasound; ICG-FA, fluorescence angiography of indocyanine green; SIRT, static infrared thermography; SIEV, superficial inferior epigastric vein.

did not find a correlation between the localization of skin blush from ICG-FA and perforator mapping with CT angiography.[14] A plausible explanation could be that they did not differentiate between fluorescence area and first appearing fluorescence spot which appears before the "blush."

Studies have shown that blood vessels can be outlined at a depth of nearly 2 cm from the skin surface by applying ICG-FA.[8,13,15] In our study, E1 and E2 showed a subcutaneous vascular network between the first appearing fluorescence spot and associated fluorescence spots. The flow within this network reveals that the perforator has a divergent branching network producing other fluorescence spots followed by fluorescence in the subdermal plexus. This network produces the IR hotspots and IR area associated with the first appearing hotspot.

Although the patterns of ICG-FA and IRT were comparable in our study, the areas of intensity were slightly different in size. In ICG-FA, fluorescence of plasma bound ICG is registered and provides direct information on intravascular perfusion. On the other hand, IRT is an indirect method to monitor perfusion and may result in an overestimation of tissue perfusion as it registers the convective heat produced by transport of warm blood. This can explain the differences in area between both imaging modalities. The rapid washout of ICG-FA could even result in a slight underestimation of the perfusion area. In 2 experimental studies evaluating skin perfusion using both imaging modalities, Miland et al came to the same conclusion.[16,17]

The flow characteristics of the selected perforator changed after the number of perforators was reduced. This was especially evident with IRT, which showed an increased IR radiation at the hotspots of the selected perforator. ICG-FA also showed increased fluorescence with a clearer border of the branching network (Figs. 3–7). This may be caused by an increased flow through the selected perforator from the source artery after other perforators have been cut and sealed.

Selecting the largest perforator with the most optimal 3-dimensional branching within the subcutaneous fat has

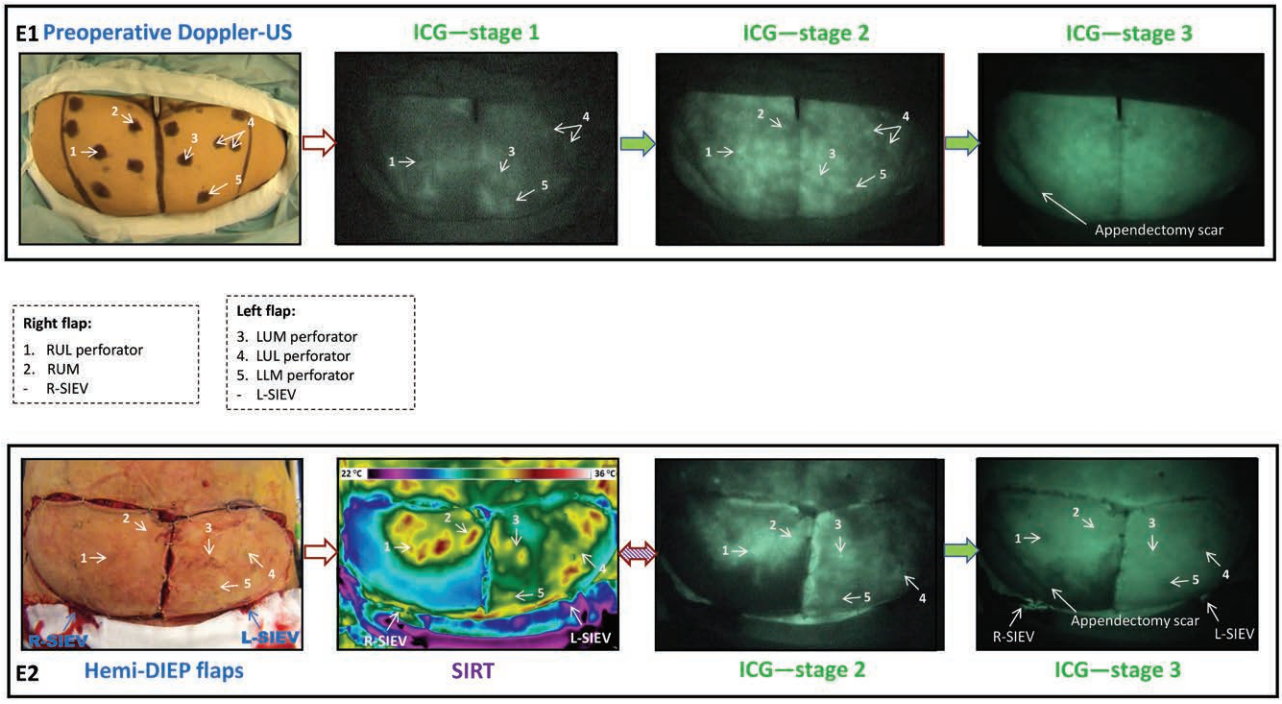

Fig. 6. An example of in vivo changes in perfusion pattern after perforator dissection in a 56-year-old female patient who had a McBurney scar and a scar after caesarean section. Each dominant perforator is identified with a white number and an abbreviation (dashed line framed box in centre of the figure). Upper row: The dynamic ICG-FA images in E1 with the first appearing fluorescence spots (stage 1) with their branching network and associated fluorescence spots, which appear slightly later (stage 2). Fluorescence spots were associated with locations of arterial Doppler sounds (white arrows). ICG-FA visualized short lasting pattern of interconnecting vessels, before the dye reached into the subdermal plexus and spread further in the entire skin (stage 3). Note the dark line at the McBurrney scar in the right lower quadrant in stage 3. Lower row: Changes in perfusion pattern on SIRT and ICG-FA after perforator dissection for each hemi-DIEP flap. The area inferolateral to the McBurney scar had low IR radiation and low fluorescence uptake. Clinical signs did not indicate any impaired perfusion in this area. The hypo-fluorescence area in the right flap also remained after the dye was draining through the open end of SIEV (stage 3). The left hemi-DIEP flap was successfully used for unilateral breast reconstruction. E1, evaluation before surgery; E2, evaluation after perforator dissection; SIRT, static infrared thermography; ICG-FA, fluorescence angiography of indocyanine green; IR, infrared; Doppler US, Doppler ultrasound; RUL, right upper lateral; RUM, right upper medial; LUM, left upper medial; LUL, left upper lateral; LLM, left lower medial; SIEV, superficial inferior epigastric vein; R, right side; L, left side.

been suggested to optimize perforator flap surgery outcomes.[18] Both ICG-FA and IRT could provide this information by, respectively, the vascular network shown by ICG-FA, and the perfusion area with associated hotspots on IRT when selected perforators are clamped.[19]

The clearly bordered area of fluorescence and IR radiation produced by the selected perforator is much smaller compared with the results of anatomical studies reported by Wong et al.[20] They showed that medial row perforators supply a larger vascular territory of tissue of 296 cm^2 compared with lateral row perforators with 196 cm^2. Lee et al explained that anatomical studies likely illustrate the maximum potential capacity of these vessels, while clinical studies incorporate hormonal or neural stimulation, which is present only in living tissue.[21] Blood vessels are of greater measurable caliber in cadaveric specimens than in the living.[22]

The results from our study were obtained during the first 2 hours of a DIEP breast reconstruction and may also explain this difference. Before surgery, perforators contribute to the perfusion of the blood vessels in the watershed zones between their perforasomes and create a pressure equilibrium that becomes disrupted with flap dissection.[21] Vessel manipulation and local accumulation of blood following ligation of perforators may further temporarily influence the flow characteristics of the selected perforator. Anatomical studies have described the existence of direct and indirect linking vessels between perforasomes.[23–25] Dahr and Taylor reported on the anatomic changes that occur at the level of the reduced-caliber choke vessels between adjacent vascular territories of a pedicled flap. Initially the choke vessels showed a vasoconstriction in the first 3 hours, but they returned to a diameter comparable to the control between 3 and 24 hours. Thereafter, the choke vessels underwent progressive sequential dilation that was most prominent between 48 and 72 hours.[25] A similar phenomenon could exist between perforasomes within the same angiosome. The pressure gradient may also be the cause of an earlier perfusion of perforasomes within the angiosome compared with perforators of adjacent angiosomes.[26] In the present study when using DIRT, clamping of a perforator resulted in an expansion of IR of an adjacent perforator to the location of the clamped perforator, indicating direct linking vessels. However, in other

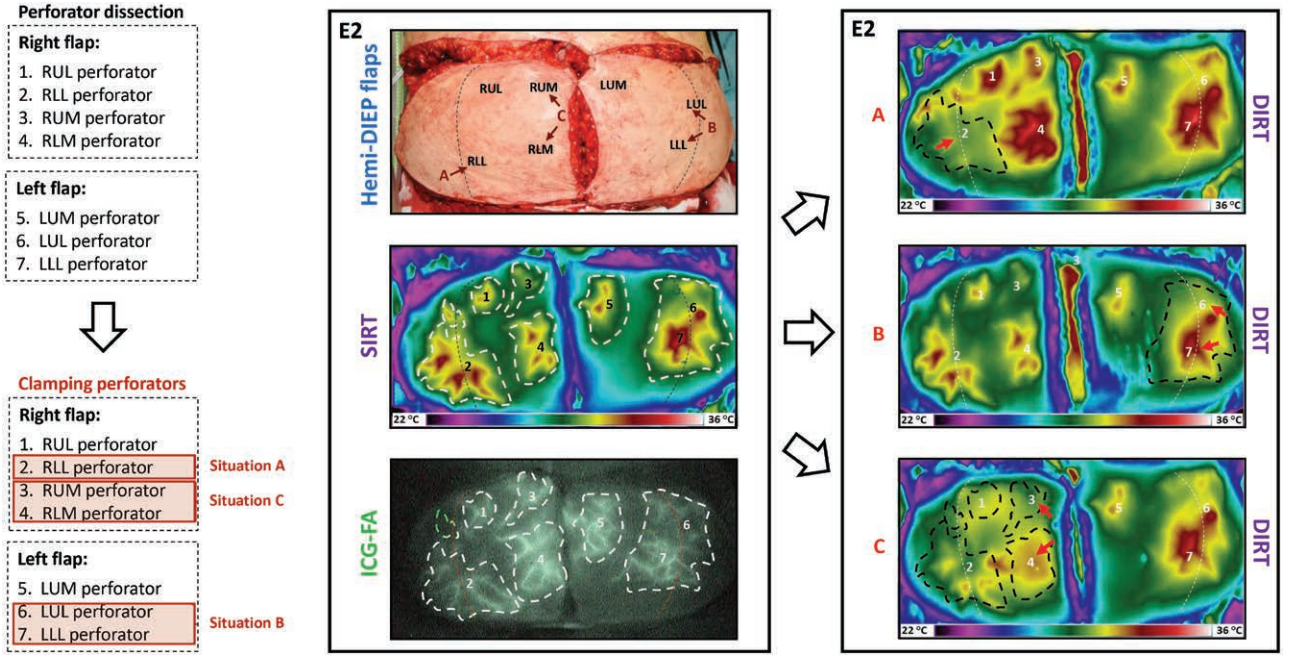

Fig. 7. Real-time perfusion images showing the dynamic effect of selective clamping of the dominant perforators in hemi-DIEP flaps of a 48-year-old woman. Left column: The upper pair of dashed line framed boxes shows abbreviations for the selected dominant perforators in both hemi-DIEP flaps after dissection. In the lower pair of dashed-lined framed boxes, the red frames identify perforators selected for clamping (situation A, B, and C). The superficial veins of both hemi-DIEP flaps were open in all situations. Middle column: A photograph of both hemi-DIEP flap with the locations of the selected dominant perforators and the perfusion patterns visualized with SIRT and ICG-FA (highlighted with dashed white lines). Dark red arrows and letters (in the photograph) indicate which perforator was selectively clamped (situation A, B, and C). Right column: Red arrows label which perforators were clamped in different situations. The changes in hotspots in DIRT (highlighted with dashed black lines) after clamping dominant perforators (situation A, B and C). Situation A: Clamping the right lateral lower (RLL) perforator resulted in a disappearance of hotspots only in the right lateral lower area, whereas the remaining lateral and medial hotspots in the right hemi-DIEP flap were more clearly visible. Situation B: Clamping the lateral perforators (LUL and LLL) in the left hemi-DIEP flap hardly changed the IR pattern of hotspots. Situation C: Clamping the right upper medial (RUM) and right lower medial (RLM) perforator resulted in weaker hotspots in that area, and the lateral perforators also became weaker. Such could indicate that the perforasomes of the medial perforators have become perfused by the lateral perforators via linking vessels. DIRT, dynamic infrared thermography; SIRT, static infrared thermography, ICG-FA, fluorescence angiography of indocyanine green; E2, intraoperative evaluation of perfusion; RUL, right upper lateral; RUM, right upper medial; RLL, right lower lateral; RLM, right lower medial; LUM left upper medial; LUL, left upper lateral; LLL, left lower lateral.

cases, no changes were monitored, which could mean the existence of indirect linking vessels (Figs. 7, 8). With the use of thermography, CTA and results from cadaveric angiographic studies, Chubb et al were able to show the robustness of interconnections between perforators.[24] A study on the perfusion dynamics of DIEP flaps showed a rapid expansion of IR hotspots within the same angiosome that could be related to the previous locations of perforators, whereas there was a clear delay in the appearance of IR hotspots in the adjacent angiosomes.[27] Such may indicate that the vascular resistance of vessels linking perforasomes within an angiosome is less than in choke vessels between angiosomes due to caliber difference. The same study also revealed a stepwise progression of perfusion of the subdermal plexus and subcutaneous tissue, each with its own time sequences. Both ICG-FA and DIRT indicate that the subdermal plexus becomes perfused after the selected perforator but before the subcutaneous network of adjacent perforators.

Another interesting finding was the lack of ICG uptake in the scar and nearby lateral area in patients previously operated on in the abdomen. IR radiation was also low in these areas, but higher than the room temperature. This was more prominent on E2 and easier to distinguish on ICG-FA, which may help in intraoperative flap planning (Figs. 5, 6).

A perforasome is the vascular territory perfused by a perforator of a known source artery. However, adequate perfusion of a perforasome also relies on venous drainage. The DIEP flap can have a dual venous system: the deep inferior epigastric vein (DIEV) and the SIEV with connecting vessels between them. One of the veins might be the dominant route to drain the DIEP flap. Obstruction of this dominant vein may influence the perfusion area of the selected perforator and contribute to flap perfusion problems.[28–30] Our results show that DIRT can highlight the dynamic changes in the DIEP flap when the dominant venous route is obstructed (Fig. 8).

The limitations of our study are that only the effect of perforator dissection on skin perfusion within a hemi-DIEP flap was evaluated. However, a previous study using DIRT reported on the perfusion dynamics of DIEP flaps and SIEA flaps across the midline.[27] Another limitation of

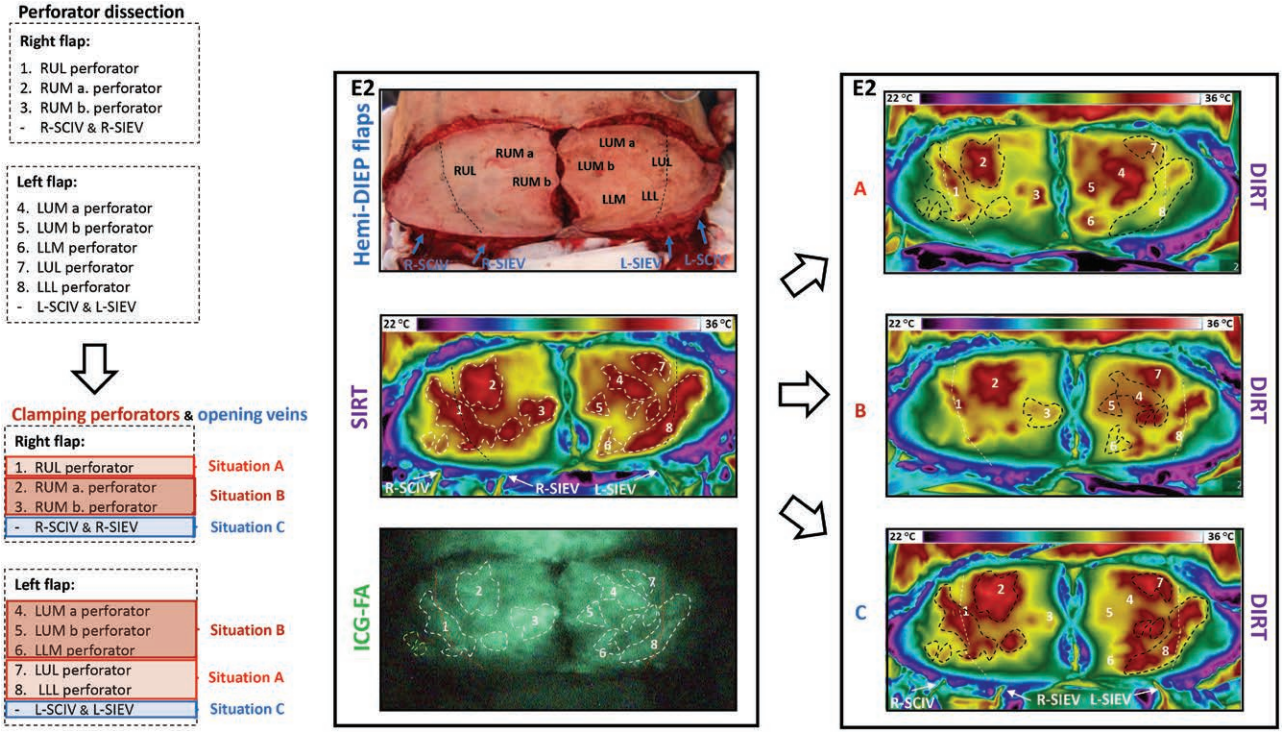

Fig. 8. Dynamic changes in perfusion following perforator dissection (E2) and clamping of blood vessel perforators in hemi-DIEP flaps of a 46-year-old woman. Left column: In the upper dashed lined framed pair of boxes, the numbers and abbreviations identify the selected dominant perforators and if the superficial veins (SCIV and SIEV) were dissected for each flap. In the lower dashed lined pair of framed boxes with red and blue frames are situations with clamping of the dissected blood vessels (situation A, B, and C shown in right box of DIRT images). Middle column: Locations of the dissected perforators and the superficial veins in both hemi-DIEP flaps. Their respective perfusion patterns visualized with SIRT and ICG-FA are highlighted and identified with white dashed lines and numbers, and the location of the superficial veins are indicated with white arrows. Right column: Images obtained with DIRT after clamping individual blood vessels (situation A, B, and C). Previous IR radiation borders are highlighted with dashed black lines to visualize changes after clamping. Situation A: Lateral perforators (RUL, LUL, and LLL) on each side were clamped, while the superficial veins were closed. Situation B: After reopening the lateral perforators, the medial perforators (RUM a, RUM b, LUM a, LUM b, and LLM) on each hemi-DIEP flap were clamped with subsequently closed SIEV and SCIEV on both sides. Situation C: When the superficial veins (SIEV and SCIV) were opened, the remaining hotspots became brighter in each flap. A possible explanation could be increased inflow after lowering venous pressure. Because the RUMa perforator (no. 2) had the brightest and largest IR pattern in all situations (A, B, and C), it was least influenced by clamping of the superficial veins. The flap was based on this particular single perforator, and the patient was discharged uneventfully after 6 days. E2, perioperative real time perfusion imaging; SIRT, static infrared thermography; ICG-FA, indocyanine green fluorescence angiography; DIRT, dynamic infrared thermography; RUL, right upper lateral; RUM, right upper medial; LUM, left upper medial; LUL, left upper lateral; LLM, left lower medial; LLL, left lower lateral; SIEV, superficial inferior epigastric vein; SCIV; superficial circumflex iliac vein.

our study is that ICG-FA and DIRT provide information on skin perfusion and less on perfusion of the subcutaneous tissue, which is important for evaluation of fat necrosis. The branching network and associated fluorescence spots, as well as the pattern of associated hotspots on IRT provide some information on subcutaneous perfusion. Previous studies have reported significantly lower incidence of fat necrosis and partial necrosis in a DIEP flap when ICG-FA was applied for deciding safe tissue margins.[7,31,32]

CONCLUSIONS

Perforator dissection causes dynamic changes in perforasome perfusion in a hemi-DIEP flap. These changes cannot be registered by clinical signs as skin color inspection. ICG-FA and IRT can provide the surgeon valuable information during surgery on the flow characteristics and the perforasome territory of the selected perforator after dissection, as long as the limitation and strength of both dynamic imaging tools are taken into consideration. Our study shows that evaluation of flap perfusion with the direct method ICG-FA and the indirect method IRT produce comparable and reproducible results.

Professor Louis de Weerd, MD, PhD
Department of Plastic and Reconstructive Surgery
University Hospital of North Norway
Sykehusveien 38
9038 Tromsø
Norway
E-mail: louis.deweerd@unn.no

ACKNOWLEDGMENTS

Experimental procedures involving human participants were in accordance with ethical principles of the 1964 Helsinki declaration with its later amendments or comparable ethical standards. The experimental protocol was approved by Regional Committee

for Medical and Health Research Ethics (REK Nord - approval ref.: 2017/1641). Written informed consent was obtained from all individuals participating in the study.

REFERENCES

1. Colakoglu S, Khansa I, Curtis MS, et al. Impact of complications on patient satisfaction in breast reconstruction. *Plast Reconstr Surg.* 2011;127:1428–1436.
2. Peeters WJ, Nanhekhan L, Van Ongeval C, et al. Fat necrosis in deep inferior epigastric perforator flaps: an ultrasound-based review of 202 cases. *Plast Reconstr Surg.* 2009;124:1754–1758.
3. Tan J, Ohjimi H, Takagi S, et al. Rezoning free muscle-sparing transverse rectus abdominis myocutaneous flaps based on perforasome groupings and a new understanding of the vascular architecture of the deep inferior epigastric artery-based flaps. *Ann Plast Surg.* 2019;83:e59–e67.
4. Taylor GI, Palmer JH. The vascular territories (angiosomes) of the body: experimental study and clinical applications. *Br J Plast Surg.* 1987;40:113–141.
5. Saint-Cyr M, Wong C, Schaverien M, et al. Perforasome theory: vascular anatomy and clinical applications. *Plast Reconst Surg.* 2009;124:1529–1544.
6. Kiely J, Kumar M, Wade RG. The accuracy of different modalities of perforator mapping for unilateral DIEP flap breast reconstruction: a systematic review and meta-analysis. *J Plast Reconstr Aesthet Surg.* 2020;10:S1748-6815(20)30670-7.
7. Varela R, Casado-Sanchez C, Zarbakhsh S, et al. Outcomes of DIEP Flap and fluorescent angiography: a randomized controlled clinical trial. *Plast Reconstr Surg.* 2020;145:1–10.
8. Azuma R, Morimoto Y, Masumoto K, et al. Detection of skin perforators by indocyanine green fluorescence nearly infrared angiography. *Plast Reconstr Surg.* 2008;122:1062–1067.
9. Verstockt J, Thiessen F, Cloostermans B, et al. DIEP flap breast reconstructions: thermographic assistance as a possibility for perforator mapping and improvement of DIEP flap quality. *Appl Opt.* 2020;59:E48–E56.
10. de Weerd L, Mercer JB, Weum S. Dynamic infrared thermography. *Clin Plast Surg.* 2011;38:277–292.
11. Muntean MV, Muntean V, Ardelean F, et al. Dynamic perfusion assessment during perforator flap surgery: an up-to-date. *Clujul Med.* 2015;88:293–297.
12. Weum S, Mercer JB, de Weerd L. Evaluation of dynamic infrared thermography as an alternative to CT angiography for perforator mapping in breast reconstruction: a clinical study. *BMC Med Imaging.* 2016;16:43.
13. Onoda S, Azumi S, Hasegawa K, et al. Preoperative identification of perforator vessels by combining MDCT, doppler flowmetry, and ICG fluorescent angiography. *Microsurgery.* 2013;33:265–269.
14. Pestana IA, Zenn MR. Correlation between abdominal perforator vessels identified with preoperative CT angiography and intraoperative fluorescent angiography in the microsurgical breast reconstruction patient. *Ann Plast Surg.* 2014;72:S144–S149.
15. Zenn MR. Fluorescent angiography. *Clin Plast Surg.* 2011;38:293–300.
16. Miland Å, de Weerd L, Weum S, Mercer JB. Visualising skin perfusion in isolated human abdominal skin flaps using dynamic infrared thermography and indocyanine green fluorescence video angiography. *Eur J Plast Surg.* 2008;31:235–242.
17. Miland Å, de Weerd L, Mercer JB. Intraoperative use of dynamic infrared thermography and indocyanine green fluorescence video angiography to predict partial skin flap loss. *Eur J Plast Surg.* 2008;30:269–276.
18. Blondeel PN. Discussion: perfusion-related complications are similar for DIEP and muscle-sparing free TRAM flaps harvested on medial or lateral deep inferior epigastric artery branch perforators for breast reconstruction. *Plast Reconstr Surg.* 2011;128:590e–592e.
19. Kalra S, Dancey A, Waters R. Intraoperative selection of dominant perforator vessel in DIEP free flaps based on perfusion strength using digital infrared thermography - a pilot study. *J Plast Reconstr Aesthet Surg.* 2007;60:1365–1368.
20. Wong C, Saint-Cyr M, Mojallal A, et al. Perforasomes of the DIEP flap: vascular anatomy of the lateral versus medial row perforators and clinical implications. *Plast Reconstr Surg.* 2010;125:772–782.
21. Lee KT, Mun GH. Perfusion of the diep flaps: a systematic review with meta-analysis. *Microsurgery.* 2018;38:98–108.
22. Rozen WM, Chubb D, Stella DL, et al. Evaluating anatomical research in surgery: a prospective comparison of cadaveric and living anatomical studies of the abdominal wall. *ANZ J Surg.* 2009;79:913–917.
23. Taylor GI, Chubb D, Ashton MW. True and 'choke' anastomoses between perforator angiosomes: part I. Anatomical location. *Plast Reconstr Surg.* 2013;132:1447–1456.
24. Chubb DP, Taylor GI, Ashton MW. True and 'choke' anastomoses between perforator angiosomes: part II. Dynamic thermographic identification. *Plast Reconstr Surg.* 2013;132:1457–1464.
25. Dhar SC, Taylor GI. The delay phenomenon: the story unfolds. *Plast Reconstr Surg.* 1999;104:2079–2091.
26. Taylor GI, Chubb D, Ashton MW. Reply: Skin perforator freeways and pathways: understanding the role of true and choke anastomoses between perforator angiosomes and their impact on skin flap planning and outcomes. *Plast Reconstr Surg.* 2014;133:720e.
27. de Weerd L, Miland AO, Mercer JB. Perfusion dynamics of free DIEP and SIEA flaps during the first postoperative week monitored with dynamic infrared thermography. *Ann Plast Surg.* 2009;62:42–47.
28. Davis CR, Jones L, Tillett RL, et al. Predicting venous congestion before DIEP breast reconstruction by identifying atypical venous connections on preoperative CTA imaging. *Microsurgery.* 2019;39:24–31.
29. Rozen WM, Pan WR, Le Roux CM, et al. The venous anatomy of the anterior abdominal wall: an anatomical and clinical study. *Plast Reconstr Surg.* 2009;124:848–853.
30. Vijayasekaran A, Mohan AT, Zhu L, et al. Anastomosis of the superficial inferior epigastric vein to the internal mammary vein to augment deep inferior artery perforator flaps. *Clin Plast Surg.* 2017;44:361–369.
31. Li K, Zhang Z, Nicoli F, et al. Application of indocyanine green in flap surgery: a systematic review. *J Reconstr Microsurg.* 2018;34:77–86.
32. Malagón-López P, Vilà J, Carrasco-López C, et al. Intraoperative indocyanine green angiography for fat necrosis reduction in the deep inferior epigastric perforator (DIEP) flap. *Aesthet Surg J.* 2019;39:NP45–NP54.